

EFFECTS OF PHOSPHATIDYLINOSITOL-3-KINASE (PI3K) INHIBITOR ON CELLULAR SIGNAL NETWORKS IN GLIOMA CELL LINES.

Naoko Iwata, Takeomi Inoue, Eiji Nishiwaki, Yasuyuki Kirii

Department of Research and Development, Carna Biosciences, Inc., BMA 3F 1-5-5 Minatojima-Minamimachi, Chuo-ku, Kobe 650-0047 Japan

Abstract

Activation of phosphoinositide 3-kinase (PI3K) signaling is commonly reported in cancer, which leads to deregulation of several intracellular processes, including cell survival, growth, proliferation and migration. PI3K activates AKT, serum/glucocorticoid regulated kinase (SGK), phosphoinositide-dependent kinase 1 (PDK1), mammalian target of rapamycin (mTOR), and several other molecules involved in cell progression and survival. It is also reported that the deletion of the gene encoding the tumor suppressor phosphatase and tensin homologue (PTEN) is one of the key factors controlling activation of the PI3K pathway.

We used RPPA to investigate the impact of PTEN on the phosphorylation status of two cells, LN229 (wt *PTEN*) and U-87 (*PTEN* deficient). As might be expected, the basal phosphorylation of most epitopes evaluated was increased in LN229 cells. The exception was NDRG1, which is a physiological substrate of SGK1. These data suggest that *PTEN* deletion affects the phosphorylation status of NDRG1 in U-87 MG cells.

Following treatment with PIK-90 for 6 hours, the phosphorylation of AKT (Ser473) and its direct substrate PRAS40 (Thr246) were decreased in both cell lines, however NDRG1 (Thr346) phosphorylation was strongly inhibited only in U-87 MG cells.

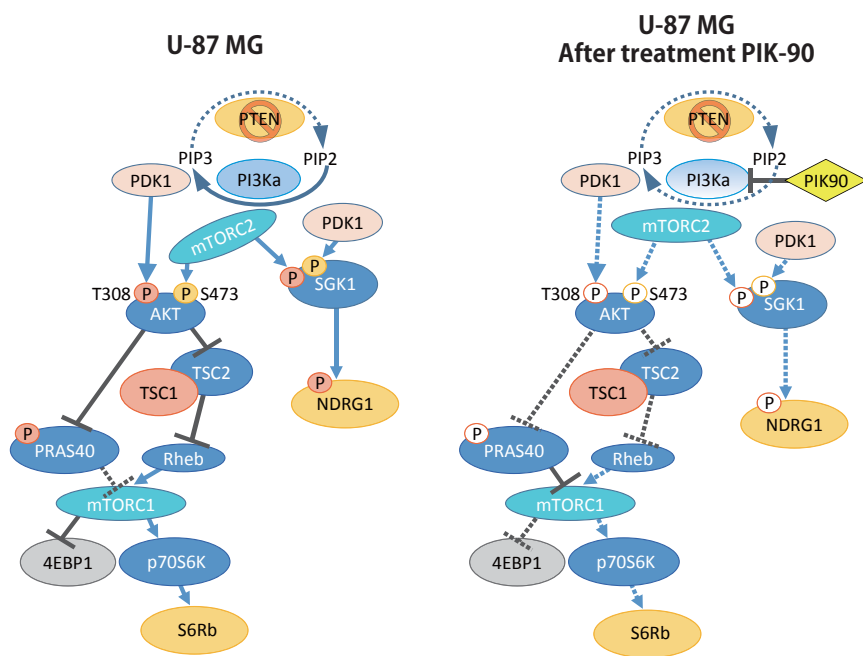


Figure 1. PI3K signaling pathway in U-87 MG cells.

Methods

Cell Culture : LN229 and U-87 MG (both human Glioblastoma) cell lines were incubated in DMEM or MEM medium (1mM sodium pyruvate) containing 10% Fetal bovine serum. Cells were treated with 0.5mM PIK-90 for 0 (before adding PIK-90), 2, 6, and 24hr (Figure 2).

PIK-90 is reported to inhibit PI3K α , PI3K β , PI3K δ , and PI3K γ with IC₅₀'s of 11nM, 350nM, 58nM, and 18nM respectively.

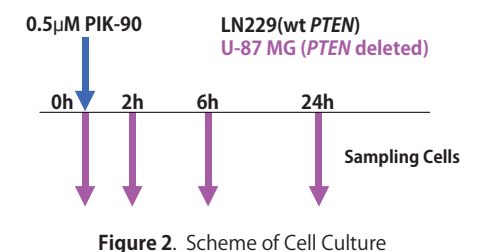


Figure 2. Scheme of Cell Culture

RPPA : 4×10^6 cells were homogenized in lysis buffer. Serially diluted lysates were spotted onto glass slides with an arrayer equipped with 32pins in order to place the expression level of samples in a dynamic range for signal detection. Each slide was probed with an anti-phospho antibody and signals were generated by employing a catalyzed signal amplification (CSA) system (Dako) and Alexa-647-conjugated streptavidin. The targets of the anti-phospho antibodies utilized in this study span a wide variety of pathways.

Data Analysis : Stained slides were scanned on a desktop scanner (InnoScan 710AL, INNOPSYS, Carbonne, France). SuperCurve (<http://bioinformatics.mdanderson.org/main/OOMPA; Overview>) algorithms were used to estimate a single value of logarithmic concentration from the four serial dilutions for each sample. Ninety-six samples were adjusted to a standardized concentration. Serial dilutions (1:2, 1:4, 1:8) were then prepared from each sample, resulting in four concentrations per sample. Each sample dilution series were then spotted in eight replicates. Two sample t-test was used for the statistical analysis and all analyses were performed using the R statistical Programming Environment (v.2.15.1).

Results

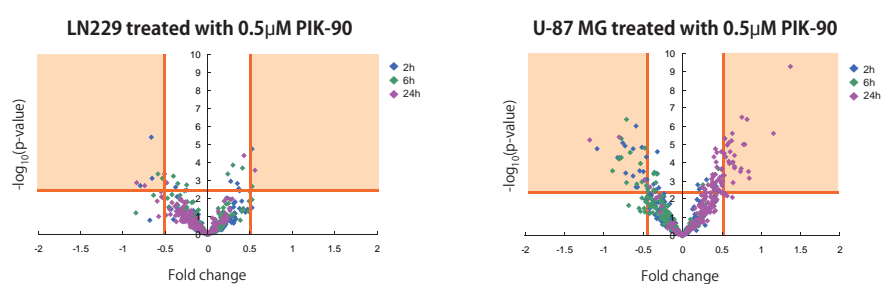


Figure 3. The p-value is plotted on the y-axis and fold change in phosphorylation content on the x-axis. Cutoff values were applied to the data as follow; >2.3 as the $-\log_{10}$ value for the p-value and $>|0.5|$ for the fold change in phosphorylation content. Using these cutoff points, the false positive discovery rate (FDR) was 10% for the LN229 data set and 2.7% for the U-87 MG data set. The shaded area contain data for which there is significant change using these criteria.

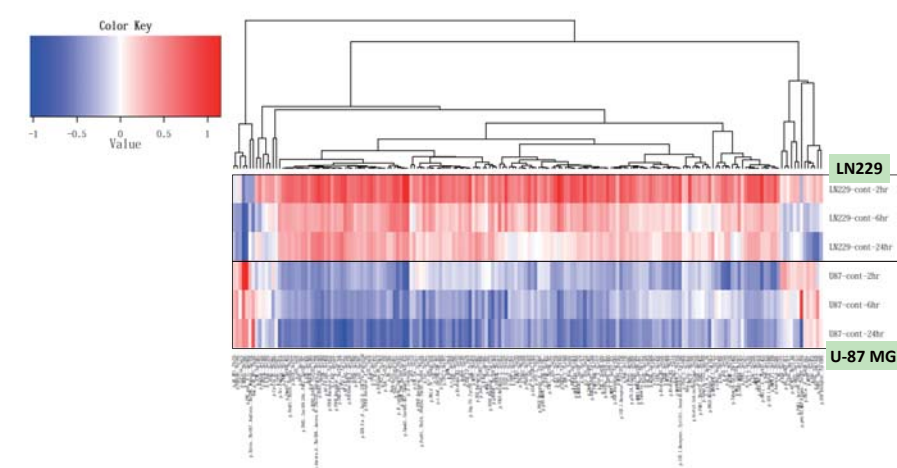


Figure 4. Basal phosphoprotein content in untreated LN229 (upper panel) and U-87 MG (lower panel) cell lines. The data is subjected to complete linkage clustering using a Pearson correlation similarity metric.

Elevated phosphorylation was detected for the following proteins in U-87 (*PTEN* deficient) cells
 p-NDRG1 (Thr346), Non p-4E BP1 (Thr46), p-4E BP1 (Thr70), p-PKC pan β II (Ser660), p-Cofilin (Ser3), p-Ezrin (Thr567), Radixin (Thr564), Moesin (Thr558), p-PRAS40 (Thr246)

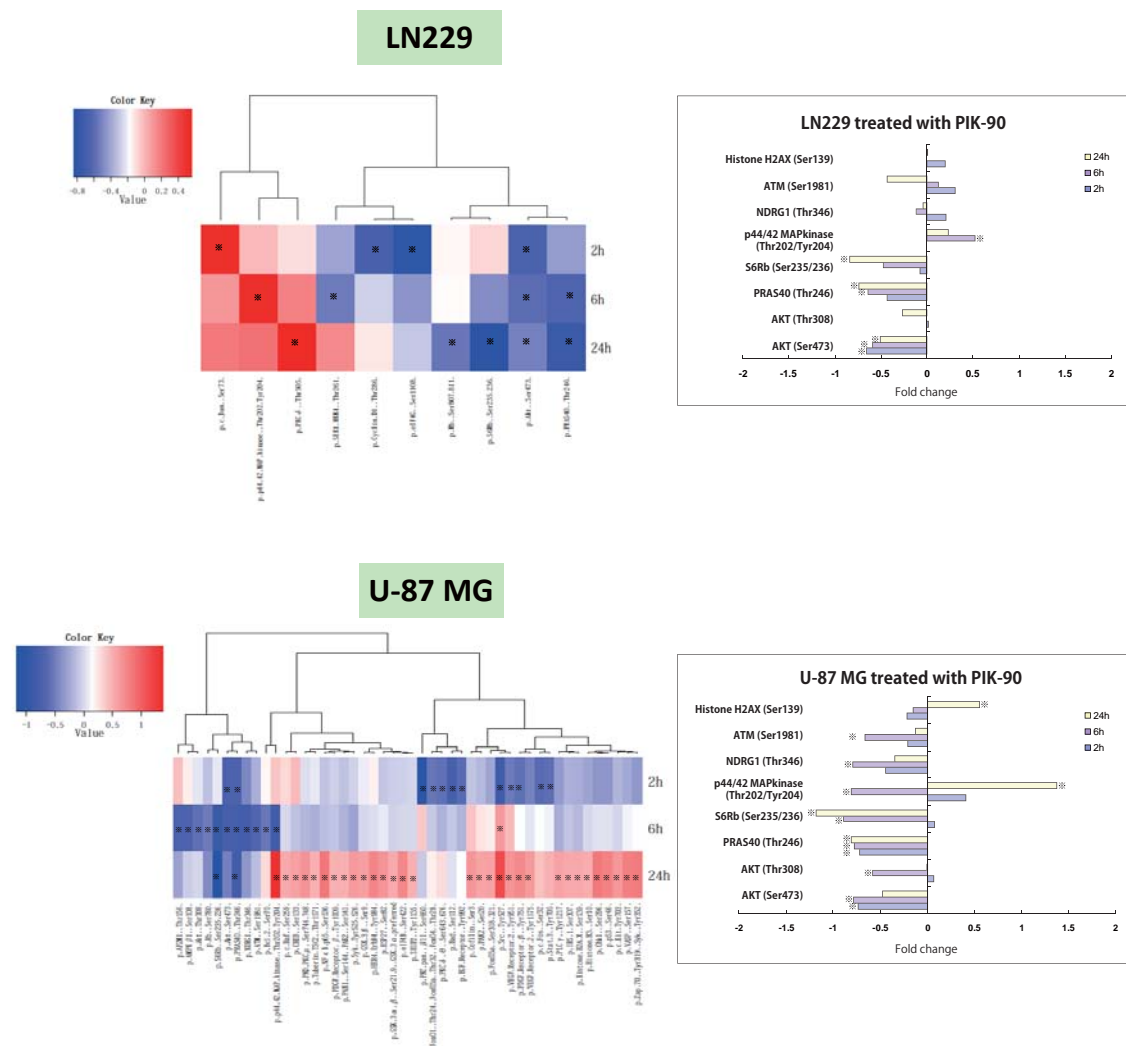


Figure 5. Heat map representation of statistically significant changes in phosphoprotein content as measured in LN229 (upper panel) and U-87 (lower panel) cells treated with PIK-90.

※ : Fold change $>|0.5|$, p-value <0.005

Conclusion

1. The basal phosphorylation levels of LN229 and U-87 MG were evaluated. The analyses revealed difference in basal phosphorylation.
2. The effects of PIK-90 on LN229 and U-87 MG phosphorylation were *PTEN* dependent.
3. Differential phosphorylation of NDRG1 may save as a biomarker for PI3K inhibitor efficacy in *PTEN* deficient cancers.